AD-A058 694 JOHN CARROLL UNIV CLEVELAND OHIO DEPT OF PHYSICS F/G 20/6
ACOUSTICALLY INDUCED PHASE AND INTENSITY MODULATION IN OPTICAL --ETC(U)
AUG 78 E F CAROME, M P SATYSHUR N00014-75-C-0247
UNCLASSIFIED PH-78-2 NL

1 OF 1
AD A058 694

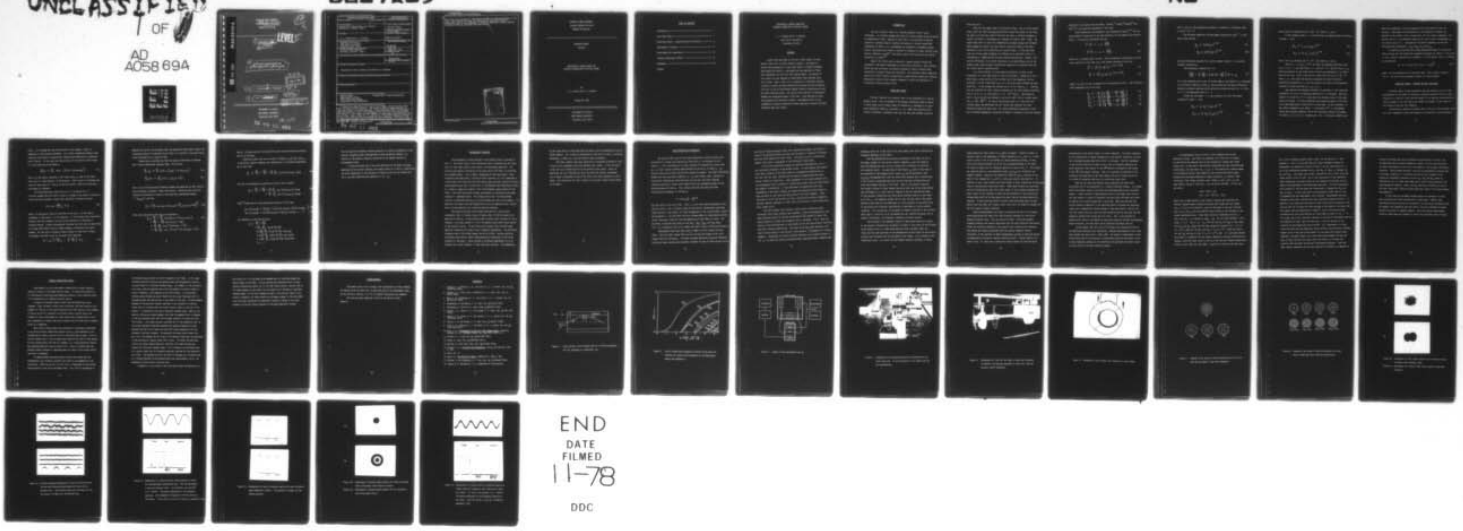

END
DATE FILMED
11-78
DDC

OFFICE OF NAVAL RESEARCH

(15) Contract N00014-75-C-0247

PROJECT NR 384-309

(12)

LEVEL II

(9) TECHNICAL REPORT,

(14) PH-78-2

(6) ACOUSTICALLY INDUCED PHASE AND INTENSITY MODULATION IN OPTICAL FIBERS,

By

(10) E. F./Carome [redacted] M. P./Satyshur

(12) 45 p.

(11) 22 Aug [redacted] 78

DEPARTMENT OF PHYSICS

JOHN CARROLL UNIVERSITY

Cleveland, Ohio 44118

SECURITY CLASSIFICATION OF THIS PAGE (When Data Entered)

REPORT DOCUMENTATION PAGE		READ INSTRUCTIONS BEFORE COMPLETING FORM
1. REPORT NUMBER	2. GOVT ACCESSION NO.	3. RECIPIENT'S CATALOG NUMBER
4. TITLE (and Subtitle) Acoustically Induced Phase and Intensity Modulation in Optical Fibers		5. TYPE OF REPORT & PERIOD COVERED Technical Report 6. PERFORMING ORG. REPORT NUMBER PH 78-2 (ONR)
7. AUTHOR(s) E. F. Carome and M. P. Satyshur		8. CONTRACT OR GRANT NUMBER(s) N00014-75-C-0247
9. PERFORMING ORGANIZATION NAME AND ADDRESS Department of Physics John Carroll University Cleveland, Ohio 44118		10. PROGRAM ELEMENT, PROJECT, TASK AREA & WORK UNIT NUMBERS NR 384-309
11. CONTROLLING OFFICE NAME AND ADDRESS Office of Naval Research Arlington, Virginia 22217		12. REPORT DATE August 22, 1978 13. NUMBER OF PAGES 44
14. MONITORING AGENCY NAME & ADDRESS(if different from Controlling Office)		15. SECURITY CLASS. (of this report) Unclassified 15a. DECLASSIFICATION/DOWNGRADING SCHEDULE

16. DISTRIBUTION STATEMENT (of this Report)

Approved for public release; distribution is unlimited

17. DISTRIBUTION STATEMENT (of the abstract entered in Block 20, if different from Report)

18. SUPPLEMENTARY NOTES

19. KEY WORDS (Continue on reverse side if necessary and identify by block number)

Optical Fibers
Acousto-Optic Effects
Fiber Optic Sonar System
Acousto-Optic Phase Modulation
Acousto-Optic Intensity Modulation

20. ABSTRACT (Continue on reverse side if necessary and identify by block number)

Studies have been made on the use of long length, low-loss optical fiber coils as direct acoustic sensors. The theory of optical mode propagation in step index fibers is briefly presented. Phase modulation theory is considered and then applied to a fiber that propagates only the first four optical modes. The results of this theory are then compared to experimental data obtained using such a fiber. When a fiber coil is exposed to a sinusoidal pressure variation in water two phase modulation processes are easily detected. The first is due to interference between directly transmitted and back and forth reflected beams.

DD FORM 1 JAN 73 1473 EDITION OF 1 NOV 65 IS OBSOLETE
S/N 0102-LF-014-6601

Unclassified
SECURITY CLASSIFICATION OF THIS PAGE (When Data Entered)

The second arises because of interference between two propagating modes in the fiber. Data obtained on these two processes are discussed in detail. Experimental data is also presented on intensity modulation effects detected in several different multimode step index fibers.

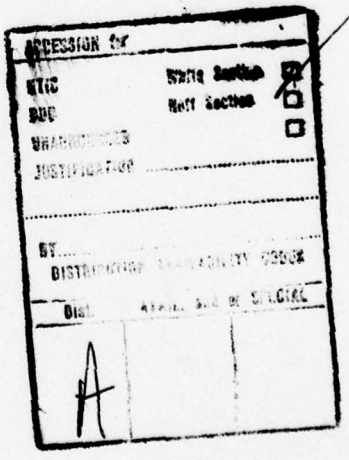

OFFICE OF NAVAL RESEARCH

Contract N00014-75-C-0247

PROJECT NR 384-309

TECHNICAL REPORT

PH 78-2

ACOUSTICALLY INDUCED PHASE AND INTENSITY MODULATION IN OPTICAL FIBERS

By

E. F. Carome and M. P. Satyshur

August 22, 1978

DEPARTMENT OF PHYSICS

JOHN CARROLL UNIVERSITY

Cleveland, Ohio 44118

TABLE OF CONTENTS

Introduction ---------- 1

Fiber Mode Theory ---------- 1

Modulation Theory - Coherent Optical Excitation ---------- 6

Experimental Procedure ---------- 11

Phase Modulation Experiments ---------- 13

Intensity Modulation Effects ---------- 21

References ---------- 25

Figures

ACOUSTICALLY INDUCED PHASE AND INTENSITY MODULATION IN OPTICAL FIBERS

E. F. Carome and M. P. Satyshur

John Carroll University

Cleveland, OH 44118

ABSTRACT

Studies have been made on the use of long length, low-loss optical fiber coils as direct acoustic sensors. The theory of optical mode propagation in step index fibers is briefly presented. Phase modulation theory is considered and then applied to a fiber that propagates only the first four optical modes. The results of this theory are then compared to experimental data obtained using such a fiber. When a fiber coil is exposed to a sinusoidal pressure variation in water two phase modulation processes are easily detected. The first is due to interference between directly transmitted and back and forth reflected beams. The second arises because of interference between two propagating modes in the fiber. Data obtained on these two processes are discussed in detail. Experimental data is also presented on intensity modulation effects detected in several different multimode step index fibers.

INTRODUCTION

The use of optical fibers is a rapidly expanding area of recent technology. It is widely assumed that they will replace copper wires and cables as communication links. Because of this, there is a great deal of applied research in progress aimed at coupling the outputs of various conventional transducers to fibers, e.g., microphones and earphones in telephone systems. Going a step beyond this, there is research in progress to couply directly from optical radiation to sound[1-5], and from a sound field directly to the optical radiation in a fiber.[6-9]

Some of the initial work on optically induced acoustic effects was performed in the Physics Department at John Carroll University. More recently, within the past two years, an extensive program of study of acousto optic interaction in optical fibers was instituted. This technical report summarizes some of the initial results on acoustically induced optical phase and intensity modulation in optical fiber elements submerged in water and subjected to a sinusoidally varying pressure field.

FIBER MODE THEORY

The basic function of an optical fiber is the transmission of electromagnetic waves. This is achieved in the typical cylindrical fiber by having an inner glass core of optical index of refraction n_1, enclosed in an outer glass cladding of index n_2, such that $n_1 > n_2$. Under this condition total internal reflection is possible, thus very low loss wave guidance along the

fiber may occur.

There are two common types of cylindrical fibers. One is called graded index, where the index increases parabolically toward the center of the fiber. The other is called step index,[10] and here the index is uniform throughout a central core which is surrounded by a cladding of slightly lower index. The graded index fiber is useful for communication purposes because the different modes propagate at nearly the same velocity along the length of the fiber, resulting in very little distortion of a pulsed signal. In the step index fiber the various modes propagate at different axial velocities, which is a disadvantage in communications and data transfer applications. However, this velocity difference is of primary importance in any application, such as the present study, where pressure induced phase modulation is examined; thus only this latter type is considered here.

It is often helpful, in a qualitative discussion, to think of the propagation in a step index guide in terms of ray optics. Referring to Fig. 1, which shows a cross section of the incident end of the waveguide, the ray indicated is called a meridional ray, i.e., one which passes through the waveguide axis. If one assumes the incident ray is in air, then $n_0 = 1$. Starting with the condition for total internal reflection at the core-cladding interface, that is $n_1 \sin \phi = n_2$, one obtains $\theta = \pi/2 - \sin^{-1}(n_2/n_1)$. Upon applying Snell's law at the air-core boundary, one has for the critical incident angle, $\sin \theta_c = (n_1^2 - n_2^2)^{1/2}$. As long as the external angle θ_i is less than this critical angle, the meridional ray will satisfy the condition for total reflection inside the fiber core. For a more quantitative analysis of fiber optic waveguide propagation, solutions of Maxwell's equations, using the boundary

conditions of the guide, must be found. Snitzer,[11] Gloge,[12] Marcuse[13] and Keck[10] all give detailed treatments of this type.

Using elementary electromagnetic wave propagation theory,[14,15] one can reduce Maxwell's equations to the wave equations for the magnetic and electric fields. In cartesian coordinates one has

$$\nabla^2 \vec{E} = \varepsilon \mu \frac{\partial^2 \vec{E}}{\partial t^2} \tag{1}$$

$$\nabla^2 \vec{H} = \varepsilon \mu \frac{\partial^2 \vec{H}}{\partial t^2} \quad , \tag{2}$$

where $\nabla\varepsilon/\varepsilon$ is assumed equal to zero. Using cylindrical coordinates, with the z-axis parallel to the fiber axis, one chooses solutions of the form

$$\vec{E} = \vec{E}(\rho, \phi)\, e^{-i(\omega t - \beta z)} \tag{3}$$

$$\vec{H} = \vec{H}(\rho, \phi)\, e^{-i(\omega t - \beta z)} \quad , \tag{4}$$

where β is equal to the z-component of the propagation vector. The transverse field components are of the form

$$E_\rho = -\frac{i}{K^2}\left[\beta \frac{\partial E_z}{\partial \rho} + \frac{\mu\omega}{\rho} \frac{\partial H_z}{\partial \phi}\right] \tag{5}$$

$$E_\phi = -\frac{i}{K^2}\left[\frac{\beta}{\rho} \frac{\partial E_z}{\partial \phi} - \mu\omega \frac{\partial H_z}{\partial \rho}\right] \tag{6}$$

$$H_\rho = -\frac{i}{K^2}\left[\beta \frac{\partial H_z}{\partial \rho} - \frac{\mu\omega}{\rho} \frac{\partial E_z}{\partial \phi}\right] \tag{7}$$

$$H_\phi = -\frac{i}{K^2}\left[\frac{\beta}{\rho} \frac{\partial H_z}{\partial \phi} + \omega\varepsilon \frac{\partial E_z}{\partial \rho}\right] \quad , \tag{8}$$

with $k = 2\pi n/\lambda$ as the propagation constant in a medium of a refractive index n, and $K^2 = k^2 - \beta^2$.

The following summarizes the development presented by Keck.[10] In the scalar form, one has

$$E_z = A F(\rho) e^{i\nu\phi} \tag{9}$$

$$H_z = B F(\rho) e^{i\nu\phi} , \tag{10}$$

and the differential equation for ϕ yields integer values of ν, to satisfy azimuthal periodicity.

The differential equation for F is

$$\frac{d^2F}{d\rho^2} + \frac{1}{\rho}\frac{dF}{d\rho} + \left[k^2 - \beta^2 - \frac{\nu^2}{\rho^2}\right] F = 0 . \tag{11}$$

For a step waveguide with a core of uniform index n_1 and radius of a, surrounded by an infinite cladding of index n_2, the solutions for the above differential equation are Bessel functions which satisfy the conditions that $F(\rho)$ is finite at $\rho = 0$, and approaches zero as $\rho \to \infty$.

Inside the core where $\rho < a$, the solutions are first kind Bessel functions of order ν. Thus

$$E_z = A J_\nu (u\rho) e^{i\nu\phi} \tag{12}$$

$$H_z = B J_\nu (u\rho) e^{i\nu\phi} , \tag{13}$$

with A and B as constants and $u^2 = (k_1^2 - \beta^2)$, where $k_1 = 2\pi n_1/\lambda$.

In the cladding, where $\rho > a$, the solutions are modified Hankel functions of order ν. Thus

$$E_z = C K_\nu (w\rho) e^{i\nu\phi} \tag{14}$$

$$H_z = D K_\nu (w\rho) e^{i\nu\phi} , \tag{15}$$

with C and D as constants and $w^2 = (\beta^2 - k_2^2)$, where $k_2 = 2\pi n_2/\lambda$.

Now as $w\rho \to \infty$, $K_\nu(w\rho) \to e^{-w\rho}$, and since the boundary conditions state $F(\rho) \to 0$ as $\rho \to \infty$, one sees that $w > 0$. Since $w^2 = \beta^2 - k_2^2$ this gives $\beta \geq k_2$, where the equality is the cutoff point at which the propagation is no longer bound to the core. Since u must be real inside the core, and $u^2 = k_1^2 - \beta^2$, then $k_1 \geq \beta$. Here again the equality represents the cutoff condition. Combining the conditions on β, one then obtains the range of the propagation constant for bound solutions as, $k_2 \leq \beta \leq k_1$.

Upon applying the boundary conditions of continuity of the tangential components of E and H, an eigenvalue equation for β is obtained. When this equation is solved for β it is found that only discrete values in the above range are allowed. This then determines the propagating modes in the fiber. The allowed modes may be classified in various ways. As Keck indicates, in the radially symmetric case, where $\nu = 0$ and hence $e^{i\nu\phi} = 1$, one obtains either the transverse magnetic (TM) or the transverse electric (TE) modes, for which $H_z = 0$, or $E_z = 0$, respectively. For $\nu \neq 0$ one has a hybrid case

where the z-component of both the magnetic and of the electric field are non-zero. These modes are designated HE or EH, depending on whether the magnetic or the electric field, respectively, has the larger z-component. For a given value of ν the eigenvalue equation will have m roots corresponding to the various zeros of J_ν. Combined with the above statements, one has the *following mode designations:* TE_{0m}, TM_{0m}, $HE_{\nu m}$ and $EH_{\nu m}$.

To graphically determine the allowed propagating modes of a particular fiber, one may plot the normalized propagation constant β/k, where $\beta = 2\pi/\lambda_z$ and $k = 2\pi/\lambda$, versus a characteristic parameter, V, of the guide. Here V is defined by the equation,

$$V = (2\pi a/\lambda)\,(n_1^2 - n_2^2)^{1/2}\,, \tag{16}$$

where λ is the wavelength of the incident light. Such a graph is shown in Fig. 2. Its use will be discussed in detail in a later section.

MODULATION THEORY - COHERENT OPTICAL EXCITATION

The above theory of mode propagation has been presented to aid in the consideration of the effect of applying an external pressure field to a fiber. Pressure on a fiber will cause various changes in its physical characteristics, such as changes of the core radius and length, and changes in the values of the indices of the core and cladding.

The particular problem of interest here is that of a fiber element, such as a coil, submerged in water and exposed to a sinusoidally varying acoustic

field. It is assumed that the cross section of the element is small in comparison to the acoustic wavelength. For a fiber propagating coherent laser radiation, the process of acoustically induced phase modulation is considered here in detail. In this case the time variation of the electric field vector of a given mode may be expressed as

$$\vec{E}(t) = \vec{E}_o \exp i[\omega_o t + A \sin \omega_s t] \quad . \tag{17}$$

Here ω_0 is the angular frequency of the light source, ω_s that of the sound field, and A is some function of the pressure. Again, note it is assumed here that the light source is a laser, so that the optical radiation fields have a high degree of coherence.

For phase modulation, both Cole et al.,[9] and Bucaro et al.,[7] initially assumed that the effect is due to a change in the index of refraction of the core and considered a phase shift amplitude A defined as follows

$$A = k \left(\frac{\partial n}{\partial P}\right)_s P \ell \quad , \tag{18}$$

where n is the optical index of refraction of the core, k is the optical wavenumber in free space, P is the pressure, ℓ is the acousto-optic interaction length of the fiber element, and the partial derivative is evaluated at constant entropy. Further consideration indicates that this must be generalized to include other effects such as length changes, and possibly even radius changes. For the case of pressure induced changes of index and of length, for example, one might write for the phase shift amplitude

$$A = k \left[\left(\frac{\partial n}{\partial P}\right)_s + \frac{n}{\ell} \frac{d\ell}{dP}\right] P \ell \quad . \tag{19}$$

Whatever the form of the bracketed term, the phase shift amplitude A enters the succeeding analysis in identical ways so that it is possible to proceed without being concerned with its specific form.

Assume that on exciting the fiber the phase shifted beam is combined with a second unmodulated reference beam. Thus one has

$$\vec{E}_1(t) = \vec{E}_1 \exp i\left[\omega_0 t + A \sin \omega_s t\right] \tag{20}$$

$$\vec{E}_2(t) = \vec{E}_2 \exp i\left[\omega_0 t + \phi\right] \tag{21}$$

Here ϕ is an arbitrary phase difference between the beams due to their optical path difference, assuming a single laser source. Taking the real parts and finding the intensity at a point in the resulting interference pattern $I \propto (E_{total})^2$, and thus,

$$I \propto \left[\vec{E}_1 \cos(\omega_0 t + A \sin \omega_s t) + \vec{E}_2 \cos(\omega_0 t + \phi)\right]^2 . \tag{22}$$

After some manipulation this may be transformed to

$$\begin{aligned} I \propto\ & \frac{E_1^2}{2} + \frac{E_1^2}{2} \cos(2\omega_0 t + 2A \sin \omega_s t) \\ & + \frac{E_2^2}{2} + \frac{E_2^2}{2} \cos(2\omega_0 t + 2\phi) \\ & + \vec{E}_1 \cdot \vec{E}_2 \cos(A \sin \omega_s t - \phi) \\ & + \vec{E}_1 \cdot \vec{E}_2 \cos(2\omega_0 t + A \sin \omega_s t + \phi) . \end{aligned} \tag{23}$$

Here $\vec{E}_1 \cdot \vec{E}_2$ makes explicit the possibility that the polarization directions may not be the same.

Neglecting terms that vary at angular frequency ω_0 and $2\omega_0$, since ω_0 is the optical angular frequency and undetectable in the present experiment, one is left with

$$I \propto \frac{E_1^2}{2} + \frac{E_2^2}{2} + \vec{E}_1 \cdot \vec{E}_2 \cos(A \sin \omega_s t - \phi) \quad . \tag{24}$$

This may be reexpressed by expanding the cosine term, yielding

$$I \propto \frac{E_1^2}{2} + \frac{E_2^2}{2} + \vec{E}_1 \cdot \vec{E}_2 \cos(A \sin \omega_s t) \cos\phi + \vec{E}_1 \cdot \vec{E}_2 \sin(A \sin \omega_s t) \sin\phi \quad . \tag{25}$$

Heald[16] shows that for phase modulated functions of this type,

$$\cos(u \sin\theta) = J_0(u) + 2[J_2(u) \cos 2\theta + J_4(u) \cos 4\theta + \ldots] \tag{26}$$

$$\sin(u \sin\theta) = 2[J_1(u) \sin\theta + J_3(u) \sin 3\theta + \ldots] \quad , \tag{27}$$

and therefore one may finally write

$$\begin{aligned} I \propto\ & \frac{E_1^2}{2} + \frac{E_2^2}{2} \\ & + \vec{E}_1 \cdot \vec{E}_2 \cos\phi\, J_0(A) \\ & + 2\vec{E}_1 \cdot \vec{E}_2 \sin\phi\, J_1(A) \sin \omega_s t \\ & + 2\vec{E}_1 \cdot \vec{E}_2 \cos\phi\, J_2(A) \cos 2\omega_s t \\ & + 2\vec{E}_1 \cdot \vec{E}_2 \sin\phi\, J_3(A) \sin 3\omega_s t \\ & + \ldots . \end{aligned} \tag{28}$$

Thus the resulting intensity function consists of a series of harmonics of the acoustic frequencies where the amplitude of each successive harmonic is a function of the acoustic pressure, and varies as the Bessel function of corresponding order.

It should be noted that in the case where both of the beams are phase modulated by the acoustic pressure, with phase shifts of A_1 and A_2, respectively, the final expression for the intensity is identical with Eq. 28, except that for A, one must substitute the quantity $\Delta A = A_1 - A_2$.

EXPERIMENTAL PROCEDURE

The experimental system employed in the present study is sketched in Fig. 3 The output from a 15 mw helium-neon laser is focused onto the input end of a step index optical fiber using a x10 microscope objective. The position and angular orientation of the input end of the fiber is controlled by micropositioners. Fig. 4 shows a photograph of the input setup. After traversing the fiber path, a portion of which consists of a coil submerged in a water bath, the light from the fiber again passes through a second x10 microscope objective and onto a screen with a 1 mm aperture that effectively serves as a probe to sample any region of the 15 mm diameter output pattern of the fiber. The light that passes through the aperture is directed to the photocathode of a photomultiplier. The voltage across the 1 KΩ photocathode resistor is monitored directly on an oscilloscope and with a DC voltmeter. In addition, the signal from the photomultiplier can be examined using a narrow band 3 Hz wide analyzer and a scanning spectrum analyzer.

The acoustic portion of the system consisted of a glass walled rectangular tank, 1.2 meters long, 0.4 meters wide, filled with water to a depth of 0.5 meters. A lead titanate-lead zirconate (PZT) cylinder 6.5 cm in diameter, 5 cm long, mounted in a 12.5 cm diameter brass baffle plate served as the acoustic source. It was driven by the output from a 50 watt power amplifier excited by the signal from a frequency synthesizer. The excitation frequency used in this study ranged from 10 to 30 KHz. Various receiving transducers were used to obtain semiquantatative indications of the sound intensity in the water. These included a calibrated hydrophone 2.5 cm in diameter and a small diameter (2 mm) probe type receiver. The homogeneity

of the sound field, in both amplitude and phase, could be determined using the latter element. Fig. 5 shows a photograph of, from left to right, a receiving transducer, a fiber coil, and the acoustic source transducer.

The fiber elements that were acoustically irradiated consisted of flat, circular coils suspended from large diameter wire frames. In use the plane of the coil was aligned parallel to the acoustic wave fronts. Under all conditions the coil thickness was much less than the acoustic wavelength. Fig. 6 shows a photograph of one of the fiber coils used, mounted on a wire frame. This particular coil had a radius of 4 cm with a total coiled length of 34 meters.

PHASE MODULATION EXPERIMENTS

The optical fiber used for the phase modulation studies reported here consisted of a W-type step index glass fiber with a 5 μm diameter core of index $n_1 = 1.46$, surrounded by an inner cladding of thickness 25 μm and index $n_2 < n_1$, and a second cladding approximately 30 μm thick, of index $n_3 > n_2$. Finally there was an outer thin plastic protective sheath. The index differences between the core and inner cladding, $n_1 - n_2$, was $0.006 \pm .002$. Analysis of the optical transmission characteristics of the core and inner cladding indicates that such a fiber would support only four propagating modes at the He-Ne wavelength of 633 nm. This follows from the fact that the fiber characteristic parameter V, defined by

$$V = 2\pi a/\lambda_o (n_1^2 - n_2^2)^{1/2},$$

has the value 3.1 for this fiber. Here λ_o is the free space wavelength of the optical source. Fig. 2 contains plots of the optical transmission velocities along the axis of the fiber, for light propagating in the various modes, versus the parameter V. For any fiber the only allowed modes are those whose velocity curves intersect a vertical line corresponding to that fiber's V value. For the fiber considered here these are the HE_{11}, TE_{01}, TM_{01}, and HE_{21} modes. Fig. 7 is a diagram of the first 4 modes and their electric field polarizations.

Measurements have been made using a number of coils formed from this fiber. The coil radii ranged from 2 cm to 4 cm and the length of the coils ranged from 10 to 34 meters. Two types of phase modulation processes detected earlier by other workers were examined in detail in each of these various coils.

The first of these processes arises from interference between light which is directly transmitted through the fiber and that which is internally reflected back and forth between the fiber's ends. The second is due to interference between light that is propagated in two different allowed modes.

A third phase modulation process was observed experimentally, but it was considered extraneous in the present study. It arose because the second, outer glass cladding of the fiber acted as a propagating waveguide due to the fact that the inner cladding and the plastic sheathing both had lower optical indices of refraction. Light propagated in this guide combined with core propagated light to produce an interference pattern that had rapid spatial and temporal fluctuations. In the experiments discussed here the light propagating in the outer cladding was removed by employing various types of mode strippers at the input and output ends of the fiber elements. These consisted of 10 cm long sections of fiber, from which the plastic sheathing had been removed, immersed in a small pool of glycerine or simply coated with black enamel paint.

With the cladding light removed, highly stable relatively simple structured fiber output patterns were obtained. These corresponded well with those observed earlier by Snitzer and Osterberg [17] who studied in detail the output patterns of fibers that propagate only a few modes. Fig.8 shows the electric field distributions of these modes and the two lobe patterns resulting from their various combinations. The prime on the HE_{21} mode indicates a 90° shift of polarization in the electric field pattern, a consequence of circular symmetry. Photographs of typical patterns observed in our study are shown in Fig. 9; 9a shows the highly structured pattern obtained without cladding mode

stripping, while 9b is the type of two lobe pattern most easily obtained and frequently employed in this study.

With the photomultiplier aperture positioned at the center of one of the lobes, signals at the acoustic angular frequency ω_s and its harmonics could be detected when the coil was acoustically irradiated at relatively low intensity levels. The amplitude of the signals v_{ac} were of the order of one hundredth of the photomultiplier output v_{dc} and the modulation index (v_{ac}/v_{dc}) corresponded well with the value to be expected due to interference of the directly transmitted beam with one that had been reflected back and forth once between the ends of the fiber. Even at low acoustic intensity the harmonic content of these signals was quite high, due to the large optical path difference (i.e. twice the coil length) of the two interferring beams. At high acoustic intensities one could easily generate signals of the orders up to 100 ω_s. The harmonic content did not vary from one lobe of the output pattern to the other but the amplitude of a given harmonic at any given point in the pattern did fluctuate significantly in amplitude at a given acoustic intensity. This fluctuation is attributed to random variations in the relative phase angle ϕ, referring to Eq. 28 ,between the two interferring beams, due to thermal fluctuations, low frequency vibrations and other sources.

The increase in the harmomic content of these phase modulation signals as the acoustic intensity was increased is evident in the series of oscilloscope traces shown in Fig. 10. These were obtained using a 26 meter fiber coil. These show the time variation of the photodetector output signal as the acoustic pressure was increased from top to bottom in the figure. As is evident in the bottom most trace, which occur for the highest acoustic intensity, a second

higher modulation index signal at ω_s begins to appear. Further increase in pressure leads to the appearance of higher harmonics at 2 ω_s and 3 ω_s in this signal so that it too is attributed to a phase modulation process, in this case to the beating between two of the four propagating modes of the fiber. This type of signal and its frequency spectrum is seen in Fig. 11. This signal was characterized by a high modulation index (v_{ac}/v_{dc}) but relatively low harmonic content. Typically the modulation index for the ω_s term was of the order of 0.5, though the 3 ω_s and 4 ω_s terms were usually less than 0.1. In addition to this, these signals were very steady in time, without the fluctuations noted in the previously described signal. These three factors are consistent with the interpretation that this latter signal is due to beating between two modes, since in this instance it would be the difference in the acoustically induced phase shift of the two modes that would lead to the phase modulation observed. In this case the effective optical path difference would be much smaller than the fiber coil length, rather than twice its length as assumed for the first type of signals observed.

Detailed measurements were taken to determine the ratio of the phase shifts associated with these first two processes produced by a particular intensity acoustic wave. This was done as follows. Using the scanning frequency analyzer the spectra associated with the back reflected interference effect was carefully examined as the acoustic wave intensity was increased. Even though the signals associated with the various harmonics rapidly fluctuated, it was possible to obtain photographic records of observed spectra corresponding to particular acoustic intensity levels. Typical spectra are shown in Fig. 12. Note that a particular range of harmonics form the major

contribution to the output signal at a given intensity. The center frequency of this range moves to higher frequencies as the acoustic intensity, and thus the corresponding phase modulation level is increased. Specific components in the excited range may be made to go to zero by precisely adjusting the sound intensity; these zeroes in the $n^{\underline{th}}$ harmonic correspond to the zeroes of the $n^{\underline{th}}$ order Bessel function. Thus it is possible to determine fairly accurately the magnitude of the total phase shift ΔA by finding which pair or triplet of harmonics were zero at a particular sound level.

When the two mode interference signal appeared, the phase shift associated with it was determined in a slightly different fashion. As already noted the harmonic signals associated with mode-mode beating were extremely stable. A short section of approximately 20 cm of the output lead from the coil was placed in a water filled petri dish and either the water was cooled by adding ice or slowly heated with a hot plate. When this was done the various harmonic components in the observed spectra increased and decreased slowly due to temperature induced changes of the phase angle ϕ (see Eq. 28). This was clearly the case since the even harmonics went to zero when the odd harmonics reached their maxima and vice versa. Thus it was possible to determine the ratio of the maxima of successive harmonics and the corresponding Bessel functions, and from these ratios determine the phase shift δA.

In this manner then the ratio of the phase shift associated with the two modulation processes were determined. Repeated measurements of this type have yielded the value $\Delta A/\delta A = 1500 \pm 30\%$. The spread in experimental values arises mainly due to inaccuracies in determining precisely the zeroes in the various components because of the relatively low amplitude and poorer signal to noise ratio of the back reflected signals.

The experimental value of $\Delta A/\delta A$ is to be compared with various theoretical values. The latter are obtained, for a fiber coil of length L, by considering the expected ratio of the acoustically induced path length change $\Delta(2L)$, in the case of the directly transmitted and back reflected beam interference, with the value $\delta(L_1 - L_2)$; i.e. the acoustically induced change of the effective optical path lengths for two interferring optical modes. Assuming that the same acoustically induced processes, e.g. optical index variations, fiber length variation, etc., affect L, and L_1 and L_2 in the same fashion, values of $\Delta(2L)/\delta(L_1 - L_2)$ are easily obtained. In this case one writes

$$\Delta(2L) = f(p)\, n\, (2L)$$

$$\delta(L_1 - L_2) = f(p)\, (n_I - n_{II})L.$$

where f(p) is some function of the acoustic pressure that specifies the pressure induced change of effective optical path length per unit length. Also, n $(= \beta/k)$ is the effective index for the beams in the back reflected case, and n_I and n_{II} are the effective index values for the two modes in the second interference case. These index values are estimated using Fig. 2. Thus $\Delta(2L)/\delta(L_1 - L_2)$ reduces to $2n/(n_I - n_{II})$. For the fiber employed in this study, V = 3.1. The $\delta n = n_I - n_{II}$ value for the HE_{11} and TM_{01} or HE_{21} modes (the TM_{01} and HE_{21} modes have the same propagation constant for V = 3.1) is $3.1 \times 10^{-3} \pm 25\%$; for the HE_{11} and TE_{01} it is $2.8 \times 10^{-3} \pm 25\%$; and finally for the TE_{01} and TM_{01} or HE_{21} it is $3.0 \times 10^{-4} \pm 25\%$. It is not known exactly which mode is responsible for the signals observed in the back reflected case, however, since the index values n_1 and n_2 of the core and cladding respectively differ by only .006, the ratio $2n/(n_I - n_{II})$ varies at most by 10% when using

any of the 3 different possible index values for the value of n. Thus assuming n = 1.46 it can be seen that the closest agreement between the experimental and theoretical ratios of $\Delta A/\delta A$ is for the cases where δA is due to the interference between the HE_{11} and TM_{01} (or HE_{21}), or between the HE_{11} and TE_{01}. The former case yields a theoretical ratio of 940, while the latter yields a ratio of 1040. Due to the inaccuracies in the theoretical index differences, the above ratios can vary enough to bring them into the range of the experimental ratio mentioned previously. The third theoretical ratio possible is the case where the interference is between the TE_{01} and TM_{01} (or HE_{21}). In this case $\Delta A/\delta A$ is approximately 10,000, which is not in agreement with the experimental ratio obtained. Measurements were most frequently taken when a definite two lobe interference pattern occurred. In addition it was noted that the acoustic signal occurring at the center of one lobe was 180° out of phase with that observed at the center of the other lobe. This agrees with the predictions of theory[18], and as can be easily shown considering the field distributions for these modes as shown in Fig. 7. In this study, due to the limitations inherent in the type of instruments used for the injection of laser light into the fiber, it was not possible to be selective on which modes were being excited. As a consequence it is most likely that more then two modes were being excited in any particular instance. However, even if the case existed where all four modes were present simultaneously, the phase signals due to the interference between the TE_{01} and TM_{01} (or HE_{21}) would be very weak, since this effect is 10 times less sensitive then the other two possible interference processes. Since the other effects themselves are not very sensitive to pressure, as compared to

the back reflected case, and as indicated by the presence of at most, very low amplitude third and fourth harmonics, signals 1/10 this sensitive would be almost nonexistent or else lost in the signals of the stronger interference processes. Taking another approach, since we are experimentally dealing with a non-ideal situation, it is possible that due to the closeness of the theoretical propagation constants for the TE_{01}, TM_{01} and HE_{21} modes (as indicated by Fig. 2), these three modes may in reality have essentially the same propagation constant. Hence, the HE_{11} mode could interfer with any of the other three modes, producing phase modulation signals of the type observed experimentally.

In this study the agreement between theory and experiment is quite good considering the large uncertainties in both areas. However, more consideration should be given to the specifics of the various processes since, for example, the assumption that each mode is similarly effected by dynamic pressure variations is somewhat tenuous. Also, more careful measurements should be taken where one attempts to excite only particular pairs of modes.

INTENSITY MODULATION EFFECTS

Measurements have also been made of acoustically induced intensity modulation effects in multimode optical fibers. To reduce the possibility of simultaneously detecting phase modulation effects, a high intensity xenon arc was employed as an incoherent optical source.

A number of different types of step index multimode fibers were examined. These included a Valtec glass core-glass clad fiber having a core diameter of ≈100 μm; an ITT glass core-glass clad fiber having a core diameter of ≈80 μm, and an ITT concentric core fiber having a central glass core diameter of ≈60 μm surrounded by a lower index glass cladding which in turn was surrounded by a higher index glass cladding such that this outer cladding served as a waveguide.

When coils of these fibers were acoustically irradiated as described in an earlier section, modulation signals at only ω_s were detected in the photomultiplier output, even for coils of relatively small length. Coils of various lengths from .5 up to 8 meters were used but the level of the signals did not correlate well with the coil lengths, i.e. strong modulation signals were detected both with long and short coils. There is evidence that the detected signals decrease in magnitude when the length of the output lead of the fiber is increased.

In addition when the output optical pattern was probed with the photodetector, the intensity variation was found to be assymmetrical over the pattern. Referring to Fig. 13; Fig. 13a is a photograph of the focused output pattern of the Valtec multimode fiber. Fig. 13b is a photograph of

the focused output pattern of the ITT concentric core fiber. In all cases intensity modulation signals were observed when the photodetector aperture was positioned on a light-dark boundary edge. For example, in the concentric core fiber, when the aperture was at the top boundary an optical signal of angular frequency ω_s was observed on the oscilloscope. As the aperture location moved through the outer bright band the signal decreased until it disappeared when the aperture was in the center of the band. Further movement downward of the aperture location resulted in the increase of an optical signal 180° out of phase with the initial optical signal at the top of the pattern. It maximized at the inner light-dark boundary edge. Again as the aperture location was moved downward the signal disappeared only to reappear at the next boundary again 180° out of phase, making it in phase with the first signal. This phase reversal continued for all the boundaries until at the bottom outermost light-dark boundary the intensity modulation signal detected was 180° out of phase with the first signal detected at the top outermost light-dark boundary. As expected from these results there also was a null line between the two sides of the pattern along which the amplitude of the acoustically induced signal went to zero. The other two multimode single core fibers demonstrated this identical trait when the aperture scanned the light-dark boundary edges. Fig. 14 shows an oscilloscope trace of a typical signal and its frequency spectrum, observed for the concentric core fiber. The maximum value for the ratio of the peak A.C. voltage to the D.C. voltage detected by the photomultiplier was approximately .05 to .10, depending on which type of fiber was used.

Although it is not known at this time exactly what the mechanism for

this effect is, it is believed to be somehow due to a coupling between the optical modes in the fiber. In any case the main characteristics of these intensity modulation signals are (1) the 180° phase reversal from one side of the output pattern to the other; (2) the signals are a maximum at light-dark boundary edges; (3) the only frequency present in the optical signal is the acoustic frequency; (4) these signals are extremely steady in time and appear to be relatively unaffected by temperature changes or motion of the fiber elements, unlike the signals observed in the phase modulation section.

ACKNOWLEDGMENTS

The authors would like to express their appreciation to Peter Schmidt and Charles Allen for their help in obtaining some of the experimental data, and to William H. Nichols, S.J. for his helpful discussions and comments.

This work has been supported in part by the Office of Naval Research.

REFERENCES

1. Carome, E. F., Moeller, C. E., and Clark, N. A., J. Acoust. Soc. Am. 40, 1462-1466 (1966).

2. Carome, E. F., Clark, N.A., and Moeller, C. E., Appl. Phy. Lett. 4 95-97 (1964).

3. Muir, T. G., Culbertson, O. R., and Clynch, J. R., J. Acoust. Soc. Am. 58 735-737 (1976).

4. Rosencwaig, A. and Gersho, A., J. Appl. Phy. 47 64-69 (1976).

5. Rosencwaig, A. and Hall, S., Anal. Chem. 47 548-549 (1975).

6. Bucaro, J. A., Dardy, H. D., and Carome, E. F., Appl. Opt. 16 1761-1762 (1977).

7. Bucaro, J. A., Dardy, H. D., and Carome, E. F., J. Acoust. Soc. Am. 62 1302-1304 (1977).

8. Bucaro, J. A. and Carome, E. F., Appl. Opt. 17 330-331 (1978).

9. Cole, J. H., Johnson, R. L., and Bhuta, D. G., J. Acoust. Soc. Am. 62 1136-1138 (1977).

10. Keck, D. B., Fundamentals of Optical Fiber Communication, edited by Barnoski, M. K., (Academic Press, Inc., New York, 1976) p. 1.

11. Snitzer, E., J. Opt. Soc. Am. 51 491-498 (1961).

12. Gloge, D., Appl. Opt. 10 2252-2445 (1971).

13. Marcuse, D., Bell Syst. Tech. Joul. 52 817-842 (1973).

14. Jackson, J. D., Classical Electrodynamics, (Wiley, 2nd edition, 1975) p. 334.

15. Keck, ref. 10.

16. Heald, E., The Physics of Waves, (McGraw Hill, 1969) p. 428.

17. Snitzer, E. and Osterberg, H., J. Opt. Soc. Am. 51 499-505 (1961).

18. Layton, M. R. and Bucaro, J. A., (submitted for publication).

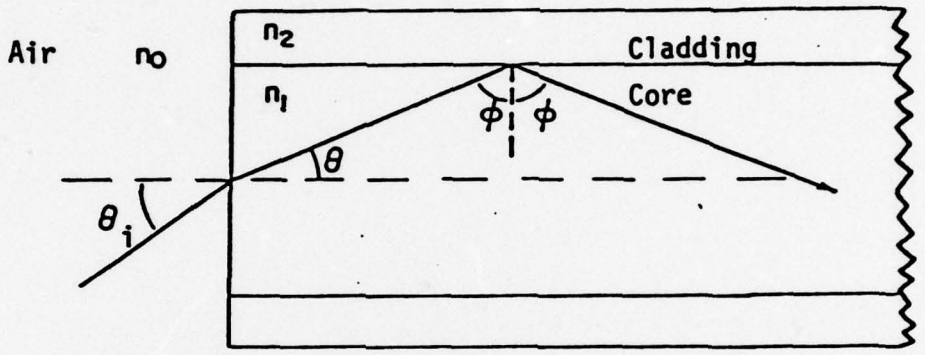

Figure 1. Cross section of the incident end of a circular waveguide. The ray indicated is a meridional ray.

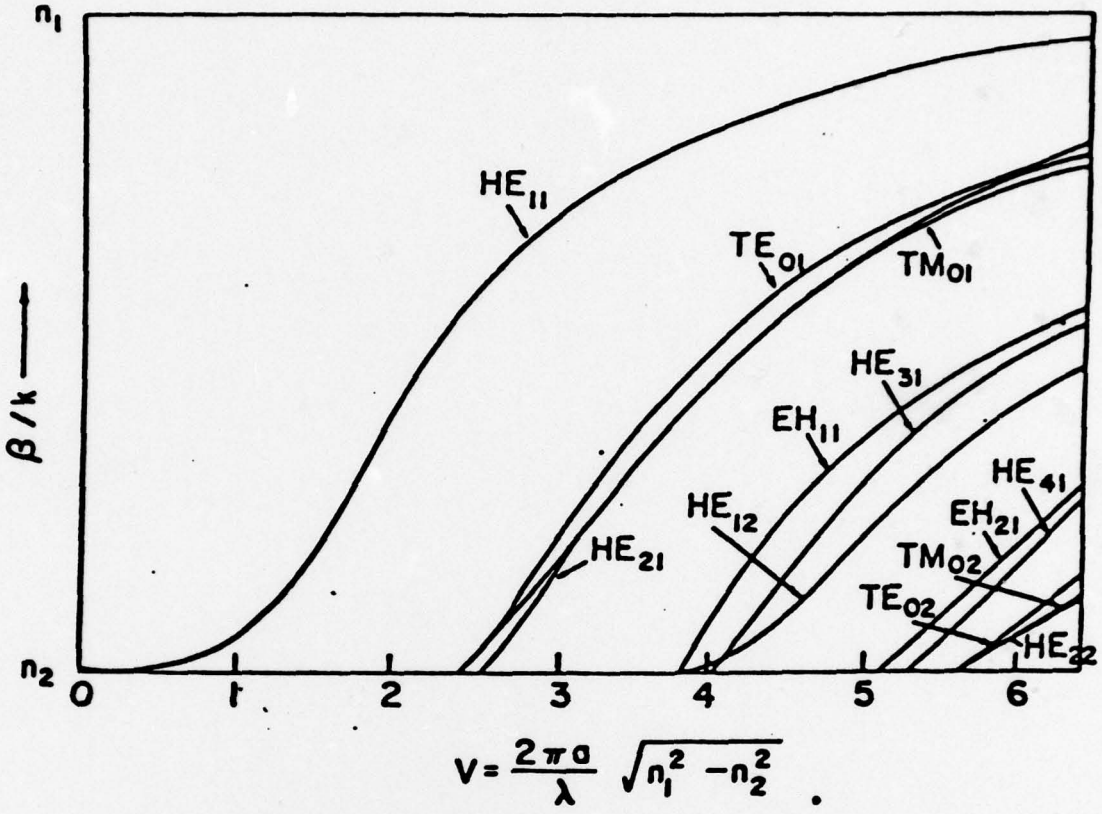

Figure 2. Plot of normalized propagation constant (from which the velocity of a mode in the waveguide can be determined) versus the parameter V.

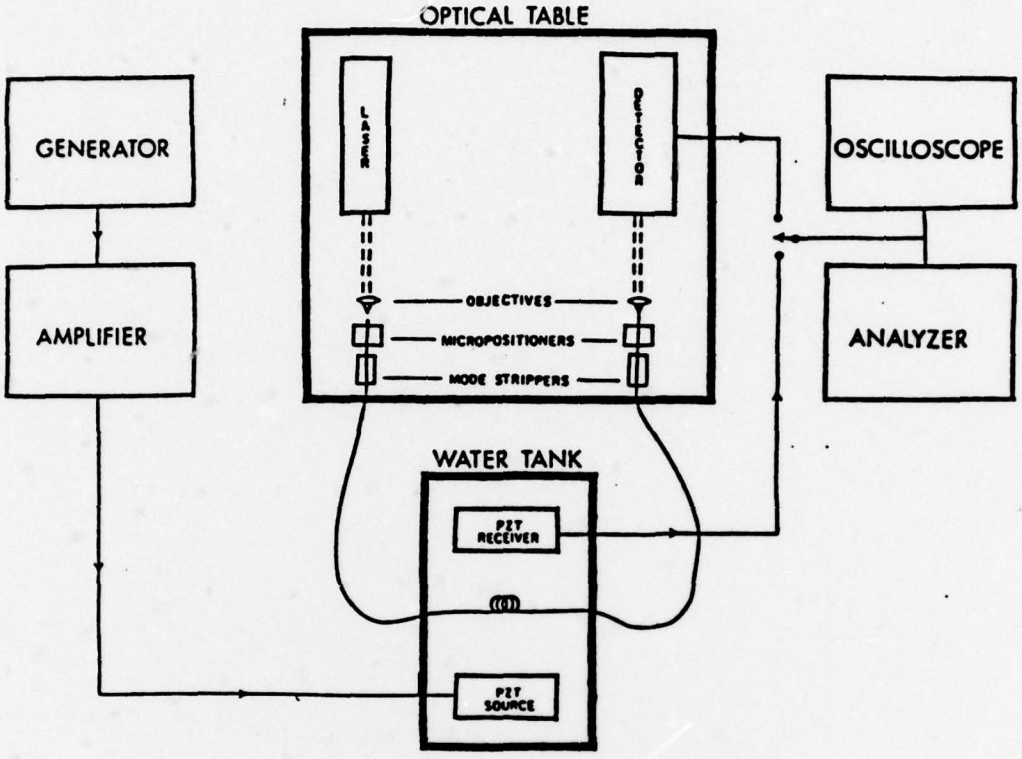

Figure 3. Sketch of the experimental set up.

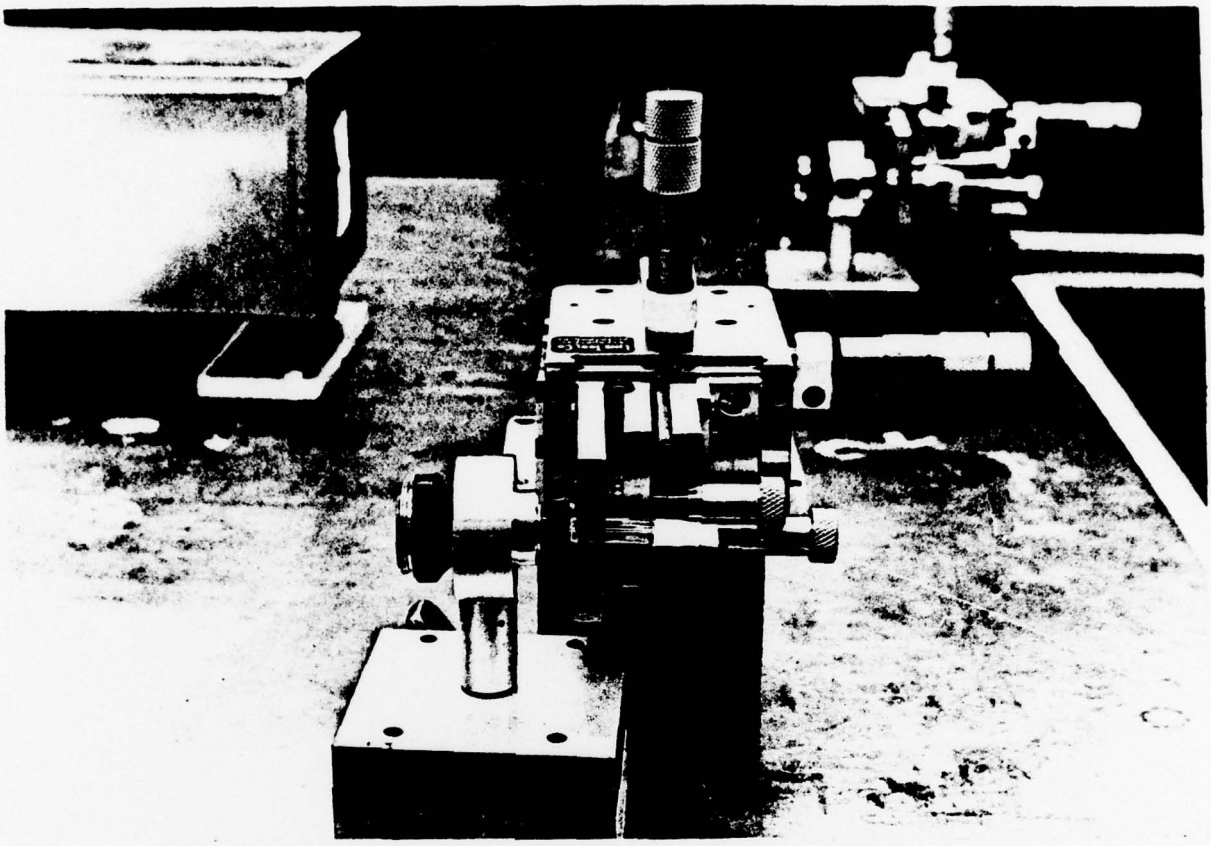

Figure 4. Photograph of microscope objective, micropositioner and fiber input end. In the background is the output end and the photodetector.

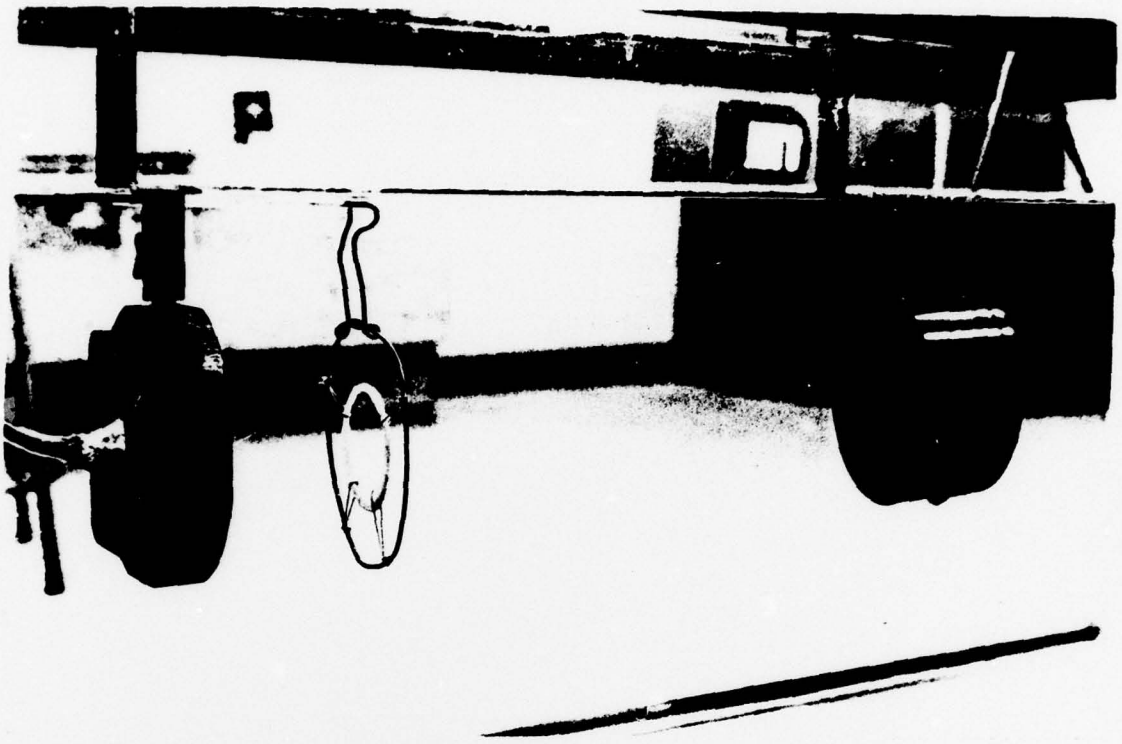

Figure 5. Photograph of, from left to right, a receiving transducer (to monitor the acoustic pressure) a fiber coil, and the acoustic source transducer.

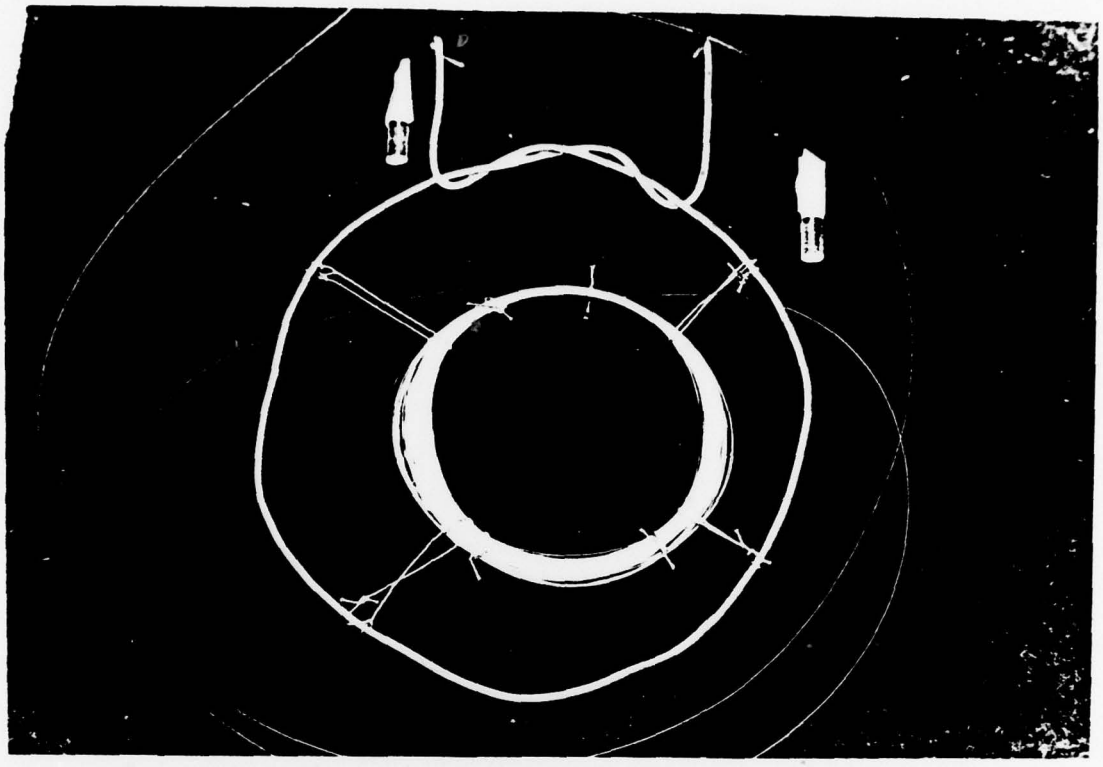

Figure 6. Photograph of the 34 meter coil mounted on a wire frame.

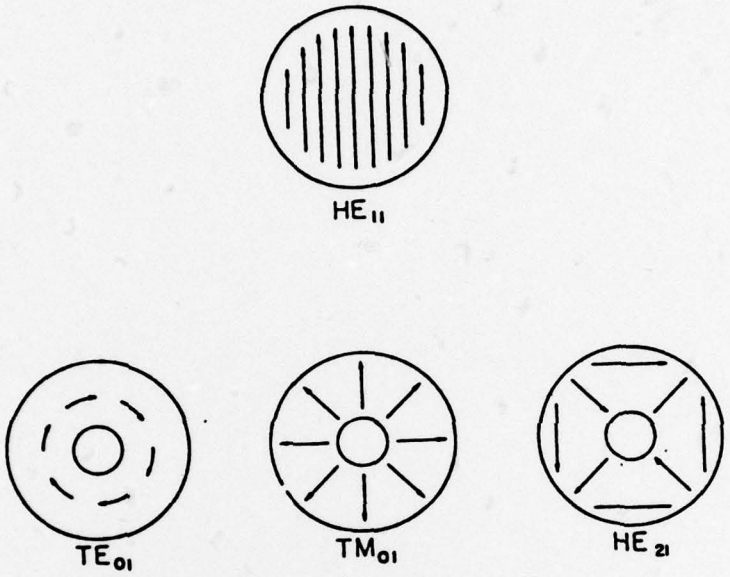

Figure 7. Diagram of the electric field distribution for the first four optical modes in the fiber waveguide.

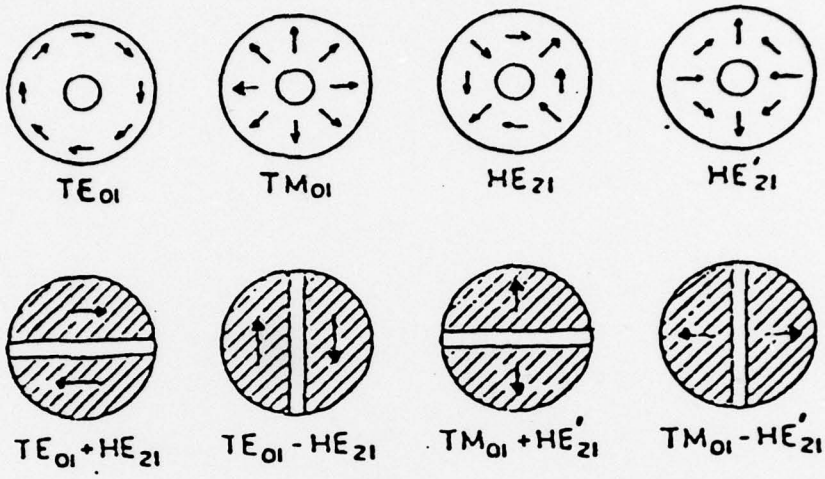

Figure 8. Diagram of the electric field distribution for three optical modes and their possible combinations.

9a

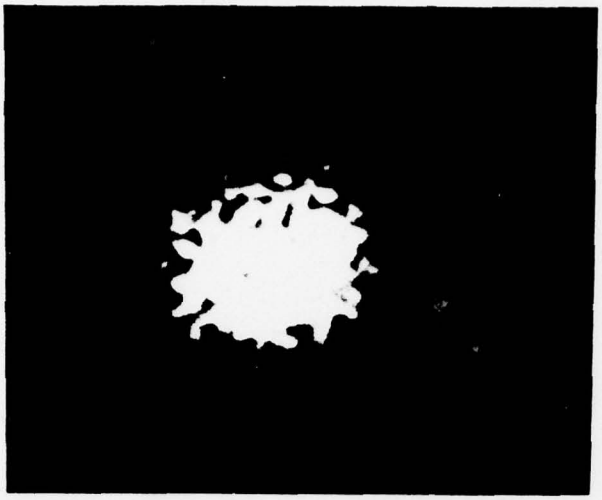

9b

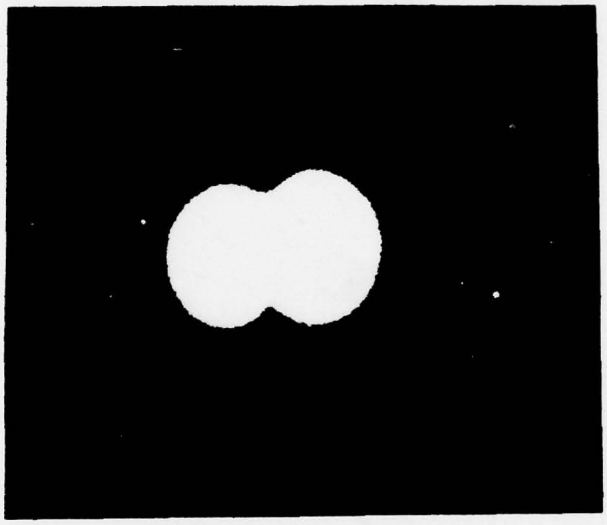

Figure 9a. Photograph of fiber output pattern with no mode stripping to remove outer cladding light.

Figure 9b. Photograph of a typical fiber output pattern using mode stripping.

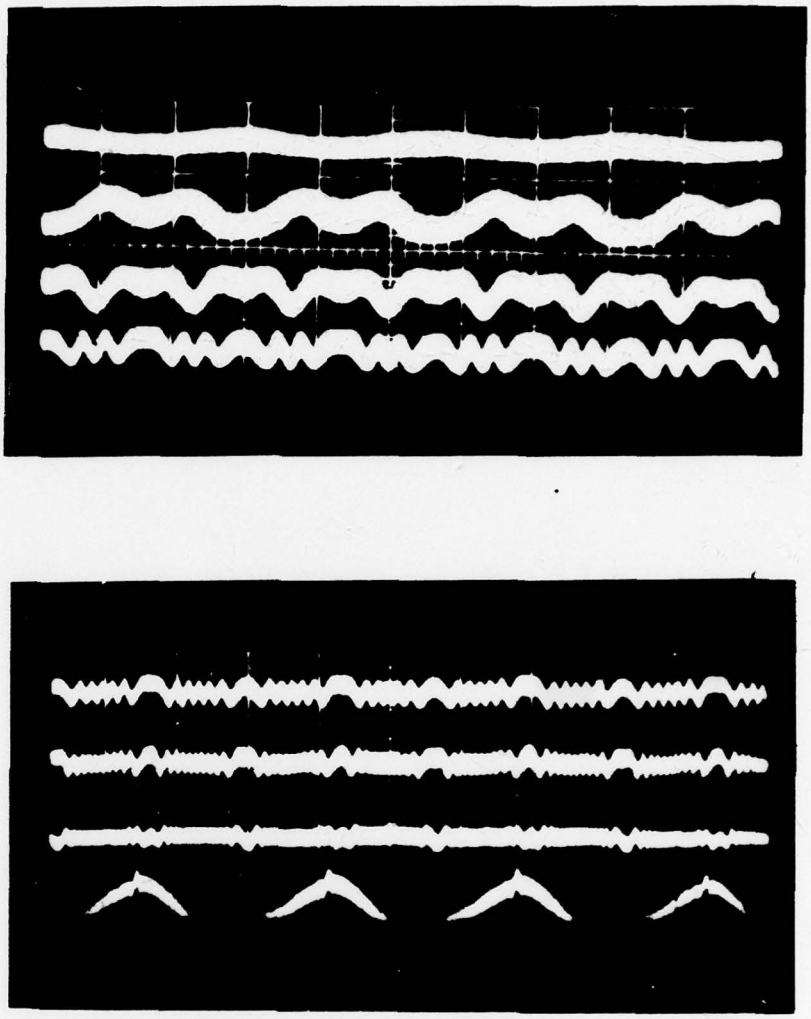

Figure 10. Multiple exposure photographs of the oscilloscope traces for the back reflected phase modulation case using a 26 meter coil. The pressure goes from .02 mbars for the top trace to 14 mbars for the bottom trace.

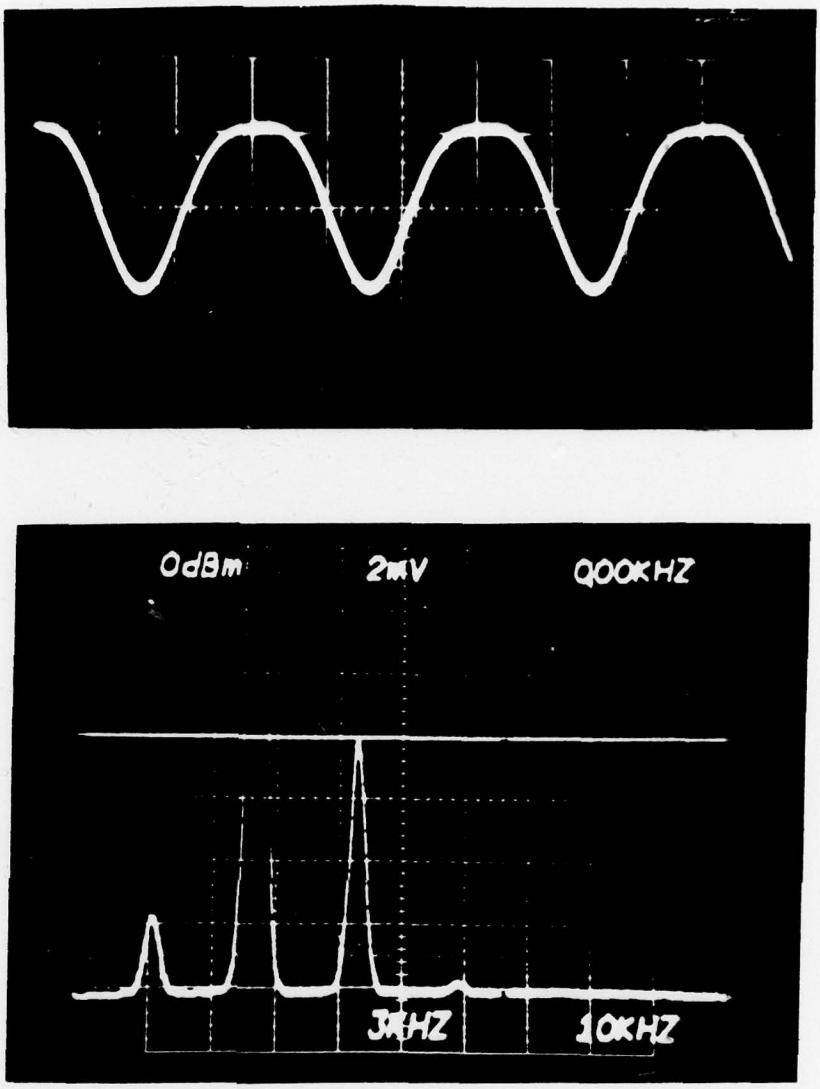

Figure 11. Photograph of a typical optical phase modulation signal for the mode-mode interference case. The top photograph is the oscilloscope trace. .05 volts/div, 20 μsec/div, D.C. = 150 mV. The bottom photograph is the frequency spectrum. The fundamental frequency is off the scope at 45 mV(rms). First spike is zero Hz, 10 KHz/div, bandwidth 3 KHz.

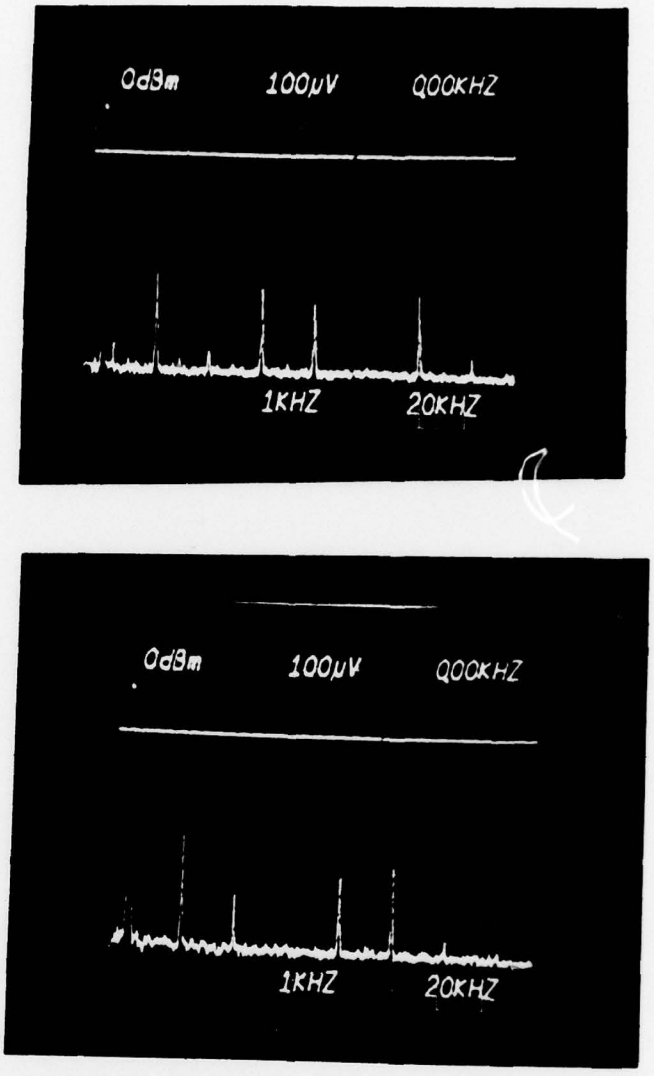

Figure 12. Photographs of typical frequency spectra for back reflected phase modulation signals. The pressure is higher for the bottom spectrum.

13a

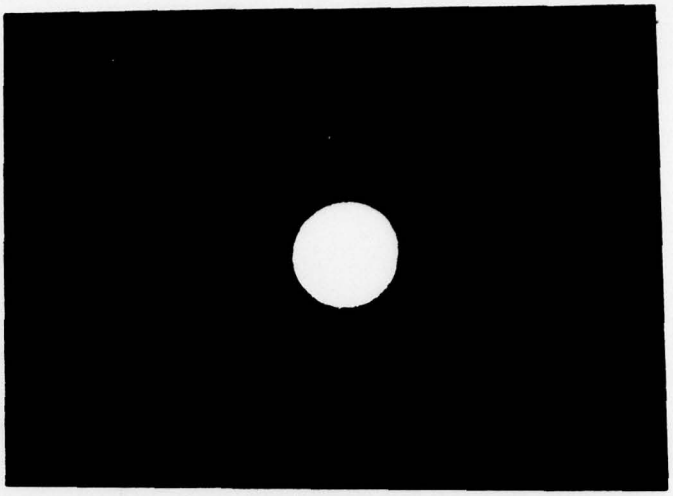

13b

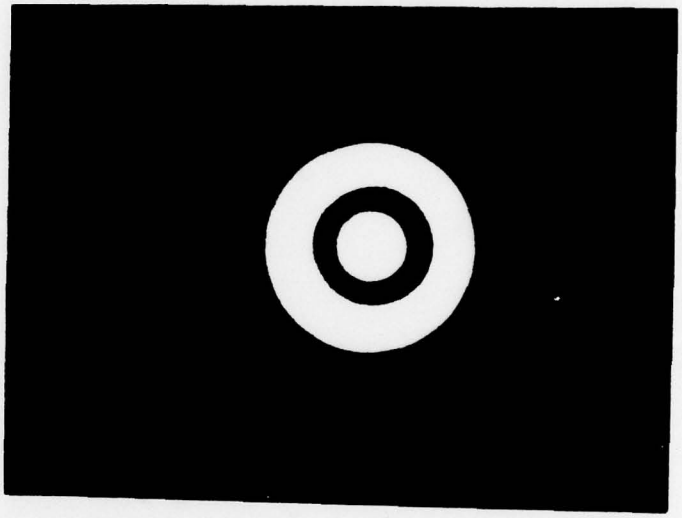

Figure 13a. Photograph of focused output pattern for Valtec multimode fiber using white light xenon arc source.

Figure 13b. Photograph of focused output pattern for ITT concentric core using xenon source.

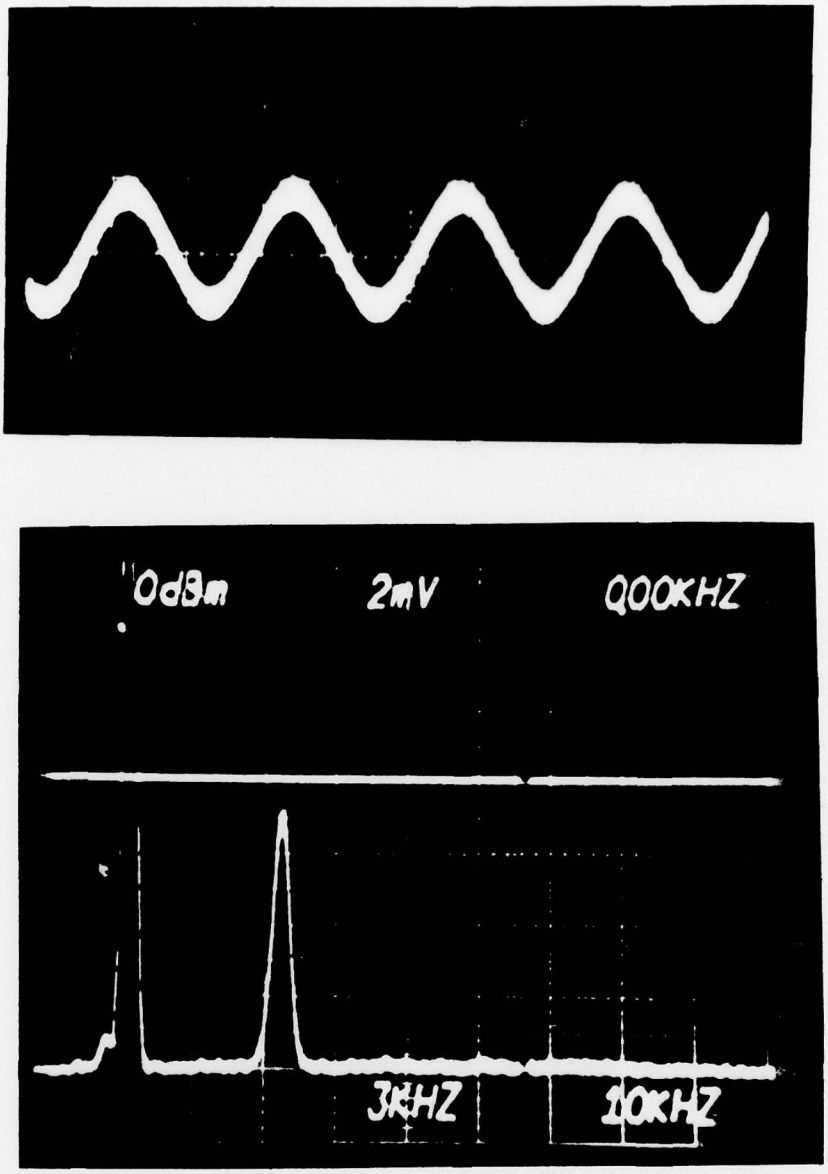

Figure 14. Photograph of a typical optical intensity modulation signal using ITT concentric core fiber and a xenon arc source. .01 v/div, 20 μsec/div, D.C. = 160 mV. The bottom photograph is the frequency spectrum in rms volts. The first spike is zero Hz, 10 KHz/div, bandwidth 3 KHz.